International Research Journal of Engineering and Technology (IRJET) e-ISSN: 2395-0056
Volume: 06 Issue: 10 | Oct 2019 www.irjet.net p-ISSN: 2395-0072

Photovoltaic Power Converter Modeling in Modelica

Montaser. A.M Qasem[1], Fouzey Aamara[2]

[1]*Department of Electrical Engineering, Faculty of Technical Sciences, Ben Walid, Libya*
[2]*Department of Electrical Engineering, Faculty of Technical Sciences, Ben Walid, Libya*

Abstract - *As the renewable energy became essential and competitive source of energy, new simulation models are needed to help comparing the feasibility of using renewable energy sources with the grid and discuss its connection and energy optimization problems in a simple and clear way. This paper presents a number of models for modelling, simulation and control of a photovoltaic system, equipped with battery and inverter to be connected to AC loads directly or to be synchronized with the electric network. The models are realized in Modelica, in order to create a useful library that compare the technical issues related to PV systems in connection with the grid and also can be integrated with similar Modelica models developed in the future.*

***Key Words*: Photovoltaic, cell, module, plant, data sheet, converter, maximum power tracking, irradiance, terrestrial solar model.**

1. INTRODUCTION

A growing demand for energy, the security of supply of fossil resources and the international agreements to mitigate climate change are key issues of modern society. These developments drastically increased the necessity of large scale implementation of renewable energy technologies over the past two decennis and will continue to do so in the near future.

This constant push to seek more innovative solutions to over-come the energy deficit and limit the negative impact on the environment. Thus, the development of non-polluting sources at the base of renewable energy is more than solicitation by both energy producers and governments.

Solar energy is a great alternative to fossil fuels and is considered an inexhaustible source of supply and is abundant. It can be easily converted into various forms of usable energy such as: thermal energy, electrical-energy, and chemical-energy.

The main applications of photovoltaic (PV) systems are in either stand-alone (water pumping, domestic and street lighting, electric vehicles, military and space applications) or grid-connected configurations (hybrid systems, power plants).

Unfortunately, PV generation systems have two major problems: the conversion efficiency of electric power generation is low (in general less than 17In General, during the photovoltaic conversion of the solar collector, heat is generated which increases the temperature of the photovoltaic cell and consequently will cause a drop in its efficiency. This phenomenon is due to the part of the solar radiation not absorbed by the cells and which is at the origin of its heating .This heating has been considered harmful for the performance of photovoltaic solar cells and several efforts have been made to evacuate this heat.

2. Photovoltaic systems modelling

2.1 Solar cell model

The term PV source is used here to refer to the device where the PV effect is taking place, from the PV cell to the PV array. As it will be shown, a single model is sufficient to model any of these devices, hence the use of this umbrella term.

One of the traditional ways to model a PV source defined in this way is to use the equivalent circuit presented in Figure (1). This is known as the single-diode circuit model of the solar cell. A two-diode model also exists, but the single-diode version provides a decent approximation and is simpler [VGF09].

The relationship between the voltages and currents in Figure (1) can be established in the form of the following equation:

$$I = I_{pv} - I_o \left[\exp\left(\frac{V + R_s I}{V_t\, a}\right) - 1\right] - \frac{V + R_s I}{R_p} \ldots\ldots\ldots (1)$$

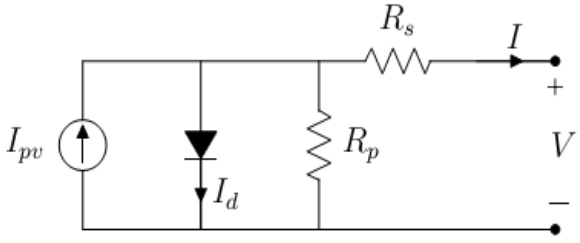

Fig.1: Equivalent circuit of a PV source

In this equation, each of the terms take the following form:

$$I_{pv} = I_{pv,n} + K_I \Delta_T \left(\frac{G}{G_n}\right) \ldots\ldots\ldots\ldots\ldots\ldots (2)$$

$$I_{pv,n} = \frac{R_p + R_s}{R_p} I_{sc,n} \ldots\ldots\ldots\ldots\ldots (3)$$

$$I_o = \frac{I_{sc,n} + K_I \Delta_T}{\exp\left(\frac{V_{oc,n} + K_V \Delta_T}{a V_t}\right) - 1} \ldots\ldots\ldots\ldots (4)$$

$$V_t = \frac{KT}{q} N_s \ldots\ldots\ldots\ldots\ldots\ldots (5)$$

$$\Delta_T = T - T_n \ldots\ldots\ldots\ldots\ldots\ldots (6)$$

Where the values of $I_{sc,n}$, K_I, K_V and $V_{oc,n}$ can be established from the data-sheet, the values of the following terms are known:

G_n = $1000W/m^2$ and T_n = 298.15K are the Standard Testing Conditions (STC) values of solar irradiation and temperature, respectively; $k = 1.3806503 \times 10{-}23\ J/K$ is the Boltzmann constant and $q = 1.60217646 \times 10{-}19\ C$ is the electric charge of the electron; N_s and N_p are the number of cells in series and in parallel, respectively; finally, G, T are the actual solar irradiation and ambient temperature, normally considered inputs to the model, and I and V are the actual panel/array current and voltage.

Figure (2) shows the I-V characteristic curves of a photovoltaic cell at a constant ambient temperature but different radiation levels.

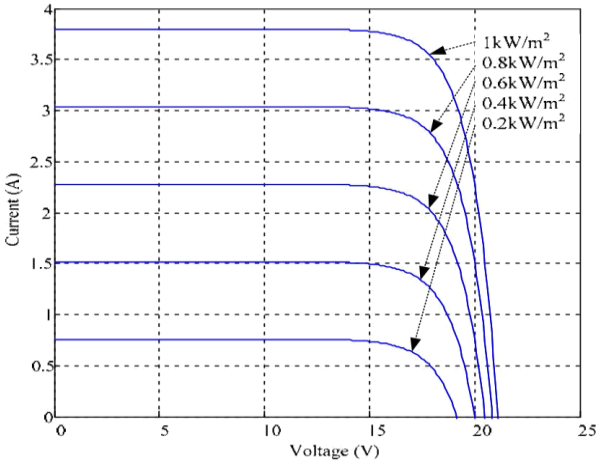

Fig .2: PV cell I-V curve at different solar radiation

While figure (3) shows the I-V characteristic curves of a photovoltaic cell at a constant solar radiation but different ambient temperature levels.

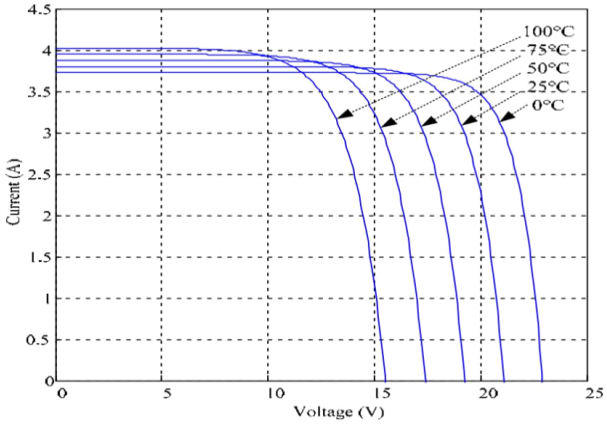

Fig .3: PV cell I-V curve at different temperature

Figure (4) shows the I-V characteristic of the solar cell for a certain ambient irradiation Ga and a certain fixed cell temperature T_c .

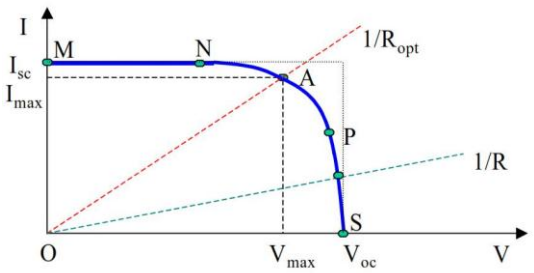

FIG.4: Typical solar cell I-V curve

In the representation of I-V characteristic, a sign convention is used, which takes as positive the current generated by the cell when the sun is shining and a positive voltage is applied on the cell's terminals.

If the cell's terminals are connected to a variable resistance R, the operating point is determined by the intersection of the I-V characteristic of the solar cell with the load I-V characteristic - see figure (4). For a resistive load, the load characteristic is a straight line with a slope I/V=1/R. It should be pointed out that the power delivered to the load depends on the value of the resistance only.

2.2 Battery

Another important element of a stand-alone PV system is the battery. Batteries are a collection of electrochemical cells. The main characteristic of the electrochemical cell is the transduction of chemical

energy into electrical energy and its reverse, thus enabling rechargeable energy storage. The battery is necessary in such a system because of the fluctuating nature of the output delivered by the PV arrays. Thus, during the hours of sunshine, the PV system is directly feeding the load, the excess electrical energy being stored in the battery. During the night, or during a period of low solar irradiation, energy is supplied to the load from the battery.

Different types of batteries exist such as the Lead-acid, Lithium ion, Nickel Cadmium, etc. The cell of any type is characterized by its open-circuit voltage, its lifetime and a cut-off voltage under which the battery will stop operating.

2.2.1 General notions for battery

Before a mathematical model for the battery is presented, some fundamental concepts of the battery are briefly reviewed:

- **Nominal capacity** C_{max} is the number of ampere-hours (Ah) that can maximally be extracted from the battery, under predetermined discharge conditions.

-State of charge SOC is the ratio between the present capacity and the nominal capacity C_{max}: **SOC**=C/C_{max}. Obviously 0≤ **SOC** ≤ 1.

If **SOC**=1 the battery is totally charged, otherwise if **SOC**=0 the battery is totally discharged.

-Charge (or discharge) regime is the parameter which reflects the relationship between the nominal capacity of a battery and the current at which it is charged (or discharged).It is expressed in hours; for example, discharge regime is 30 h for a battery 150 Ah that is discharged at 5A.

-**Efficiency** is the ratio of the charge extracted (Ah or energy) during discharge divided by the amount of charge (Ah or energy) needed to restore the initial state of charge. It is depending on the state of charge SOC and on the charging and discharging current.

-**Lifetime** is the number of cycle's charge/discharge the battery can sustain before losing 20% of its nominal capacity.

In general, the battery models view the battery as a voltage source E in series with an internal resistance, as shown in figure (5).

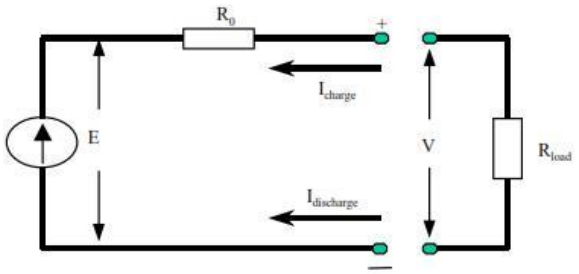

Fig.5: battery schematic diagram

where the value of the controlled voltage source, E, takes the following A decent approximation of a battery for system level studies can be created based on the circuit presented in Figure (5) where the value of the controlled voltage source, E, takes the following

$$E = E_0 - K\frac{Q}{Q - i_t} + A\,e^{-Bi_t}$$

expression:

Where E_0 is the battery constant voltage in V, K is the battery polarization voltage in V,Q is the battery capacity in Ah, it is the actual depth of discharge also in Ah, i_t is the exponential zone amplitude in V and B is the inverse of the exponential zone equivalent time constant, in $A^{-1}\,h^{-1}$

These parameters are obtained from the battery discharge curve, typically available in manufacturer's datasheets. A generic discharge curve is presented in Figure (6).

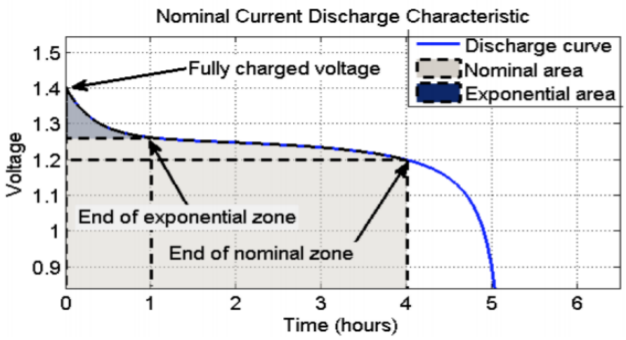

Fig .6: Generic battery discharge curve

There are different models characterizing the internal parameters of batteries but four different modelling approaches are usually adopted to study the behavior of a rechargeable electrochemical battery cell:

• Electrochemical modelling of the inner battery cell behavior;

• Stochastic modelling, in which the battery behavior is modelled using a discrete-time transient stochastic process.

• "black-box" based modelling, in which the system behavior is analytically described using a set of mathematical equations, using fuzzy logic, or artificial neural networks.

• Use of electric equivalent network models (also called equivalent circuit models), where the battery is modelled as a network of electrical components.

This approach mixed with the black box approach is adopted for this paper.

A general representation of an electrochemical accumulator cell in the equivalent circuit model is shown in figure (7).

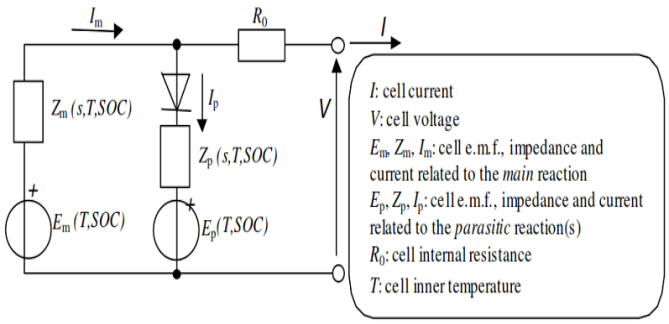

Fig .7: general electric equivalent network model of a cell taking into consideration parasitic reactions

In this figure:

The branch containing the cell electromotive force E_m, represents the main reversible reaction of the cell: the charge stored in the cell during the charge process is the time integral of the current I_m entering that branch. The electromotive force E_m is a function of the cell **SOC**, and the inner cell temperature (assumed to be uniform), T.

The branch containing the cell electromotive force E_p, represents the parasitic reactions inside the cell that are not associated with charge accumulation inside the cell. For example, in lead-acid cells, the parasitic reaction is constituted by the water electrolysis that occurs at the end of the charge process. The diode indicates that the energy always flows out of the parasitic branch. Again, the electromotive force E_p is a function of the cell **SOC**, and the inner cell temperature (assumed to be uniform), T.

The impedances are represented as functions of the laplacian transform variable s, since in this way a single Z(s) can be representative of any network of resistor and/or capacitor and/or inductor components. For instance, the network containing a resistor in series with multiple resistor-capacitor blocks, constitutes an expansion of the laplacian impedance Z(s). Both the laplacian impedances, Zm(s) and Zp(s) are functions of the cell SOC, and the inner cell temperature (assumed to be uniform), T.

2.3 INVERTER

As known, the PV arrays produce DC power and therefore when the stand-alone PV system contains an AC load, as it is the case for the inverter tied to grid system, a DC/AC conversion is required. This is thus the reason why this part briefly presents the inverter.

An inverter is a converter where the power flow is from the DC to the AC side, namely having a DC voltage, as input, it produces a desired AC voltage, as out-put – see figure (8).

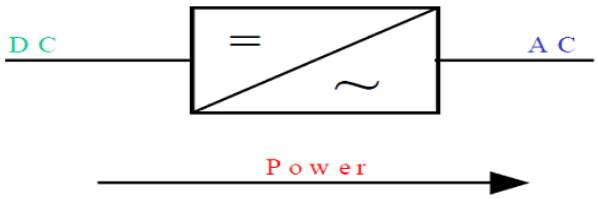

Fig.8: Connection of the inverter

The inverter is characterized by a power dependent efficiency η. The role of the inverter is to keep on the AC side the voltage constant at the rated voltage 230V and to convert the input power P_{in} into the output power P_{Out} with the best possible efficiency. The efficiency of the inverter is thus modelled as:

$$\eta = \frac{P_{out}}{P_{in}} = \frac{V_{ac} I_{ac} \cos\Phi}{V_{dc} I_{dc}} \quad , \quad I_{dc} = \frac{V_{ac} I_{ac} \cos\Phi}{V_{dc}\eta}$$

Where I_{dc} is the current required by the inverter from the DC side (for example, from the controller) in order to be able to keep the rated voltage on the AC side (for example on the load). V_{dc} is the input voltage for the inverter delivered by the DC side, for example by the controller.

3.2.1 THE THEORY OF THE THREE-PHASE GRID-CONNECTED INVERTER

The current controller of three-phase VSI plays an essential part in controlling grid-connected inverters. Consequently, the quality of the applied current controller largely influences the performance of the inverter system. Many control mechanisms have been proposed to regulate the inverter output current that is injected into the utility grid. Among these control mechanisms, three major types of current controller have evolved: hysteresis controller, predictive controller and linear proportional-integral (PI) controller. Predictive controller has a very good steady-state performance and provides a good dynamic performance. However, its performance is sensitive to system parameters. The hysteresis controller has a fast transient response, non-complex implementation and an inherent current protection. However, the hysteresis controller has some drawbacks such as variable switching frequency and high current ripples. These cause a poor current quality and introduce difficulties in the output filter design.

The PI controller is the most common control algorithm used for current error compensation. A PI controller calculates an error value as the difference between a measured inverter output current and a desired injected current to the grid, then the controller attempts to minimize the error between them. The PI controller calculation algorithm involves two separate constant

parameters, the proportional constant Kp and the integral constant Ki. The proportional term of the controller is formed by multiplying the error signal by a Kp gain.

According to the mathematical model of the grid-connected inverter, the output voltages of the inverter in the synchronous (dq) frame are given by:

$$\begin{bmatrix} u_d \\ u_q \end{bmatrix} = L\frac{d}{dt}\begin{bmatrix} i_d \\ i_q \end{bmatrix} + R\begin{bmatrix} i_d \\ i_q \end{bmatrix} + \omega L\begin{bmatrix} -i_q \\ i_d \end{bmatrix} + \begin{bmatrix} e_d \\ e_q \end{bmatrix}$$

Where ed and eq are the components of the park transformation of the grid voltage. ud and uq are the components of the park transformation of the inverter output. ω is the angular frequency of the grid. L is the inductance between the grid-connected inverter and the grid. R is the resistance between the grid-connected inverter and the grid.

The block diagram of the synchronous controller for the grid-connected inverter is represented in figure (9).

From the figure that the inverter has two PI controllers to compensate the current vector components that are defined in synchronous reference frame (dq).

Because of coordinate transformations, iq and id are DC components and therefore, PI compensators reduce the error(s) between the desired current I*d (I*q) and the actual current Id (Iq) to zero.

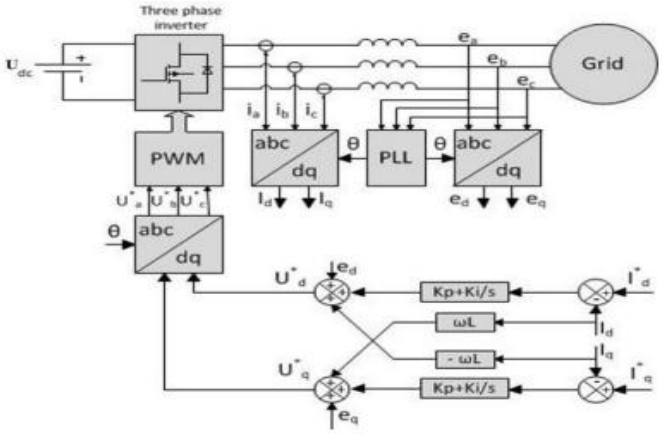

Fig .9: General structure for synchronous controller

The output energy and power factor can be controlled via changing d-axis current and q-axis current. For improving the performance of PI controller in such a structure, cross-coupling terms and voltage feed forward are usually used.

3.2.2 Space vector modulation (SVM)

SVM treats the three-phase inverter as a single unit. Specifically, in the case of a two-level inverter as shown in figure (10), there are eight possible unique states, each of which determines a voltage space vector.

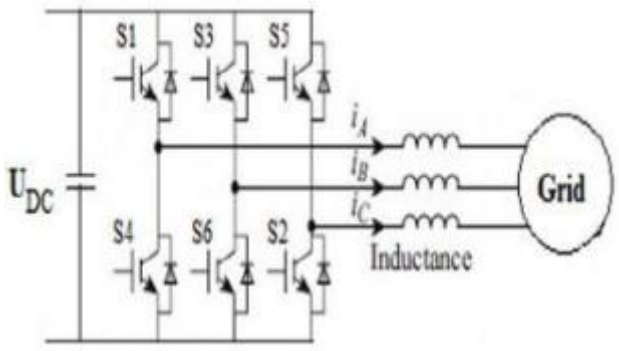

Fig.10: Two-level three-phase inverter configuration

As shown in figure (11), six voltage space vectors shape the axis of a hexagon and divide the whole space into six sectors from 1 to 6. Moreover, there are two zero vectors, U0 and U7 which lie at the origin. The angle between any two adjacent non-zero vectors is 60°. Therefore, SVM is a digital modulating technique where the objective is to find an appropriate combination of active and zero vectors to approximate a given reference voltage.

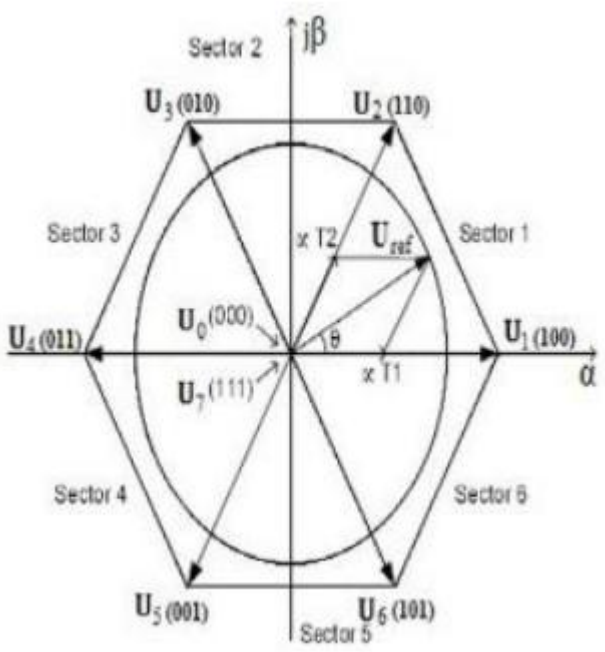

Fig.11: Six active vectors and two null vectors in SVM

In SVM, the three-phase reference voltages U*a, U*b, and U*c are mapped to the complex two-phase orthogonal (αβ) plane. This is known as the Clark's transformation.

$$\begin{bmatrix} U_\alpha \\ U_\beta \end{bmatrix} = \begin{bmatrix} 1 & -1/2 & -1/2 \\ 0 & \sqrt{3}/2 & -\sqrt{3}/2 \end{bmatrix} \begin{bmatrix} U_a^* \\ U_b^* \\ U_c^* \end{bmatrix}$$

The construction of any space vector U_{ref} which lies in the hexagon can be done by time averaging the adjacent two active space vectors and any zero vectors, as follows **:**

$$U_{ref} = \frac{U_n T_1 + U_{n+1} T_2 + U_0 T_0 + U_7 T_7}{T_s}$$

Where Un and U_{n+1} are the non-zero adjacent active vectors. U_0 and U_7 are the zero vectors. T_1, T_2, T_0, T_7 are time-shares of respective voltage vectors and T_s is the sampling period.

3.2.3 Grid synchronization

The inverter output current that is injected into the utility network must be synchronized with the grid voltage. The objective the synchronization algorithm is to extract the phase angle of the grid voltage. The feedback variables can be converted into a suitable reference frame using the extracted grid angle. Hence, the detection of the grid angle plays an essential role in the control of the grid-connected inverter.

The synchronization algorithms should respond quickly to changes in the utility grid. Moreover, they should have the ability to reject noise and the higher order harmonics. Many synchronization algorithms have been proposed to extract the phase angle of the grid voltage such as zero crossing detection, and phase-locked loop (PLL).

The simplest synchronization algorithm is the zero crossing detection. However, this method has many disadvantages such as low dynamics. In addition, it is affected by noise and higher order harmonics in the utility grid. Therefore, this method is unsuitable for applications that require consistently accurate phase angle detection.

Nowadays, the most common synchronization algorithm for extracting the phase angle of the grid voltages is the PLL. The PLL can successfully detect the phase angle of the grid voltage even in the presence of noise or higher order harmonics in the grid.

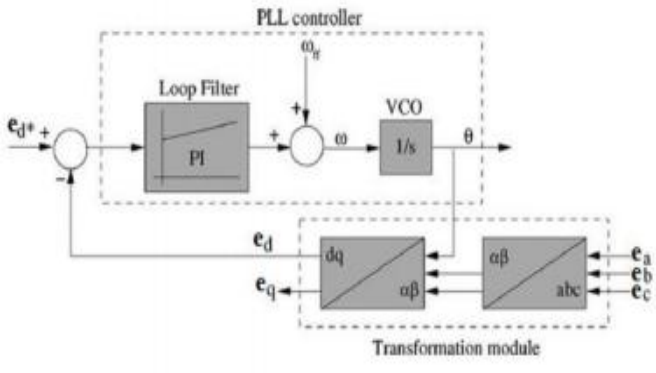

Fig .12: Basic structure of a PLL system for grid synchronization

As shown in figure (12), the PLL is implemented in synchronous (dq) reference frame. e_{abc} is the sensed grid voltage which is then transformed into DC

components using park transformation abc-dq. The PLL is locked by setting e^*_d to zero, which acts as a phase detector. A controller, usually PI, is used to control this variable, which brings the phase error to zero and acts as a loop filter. The ω_{ff} represents the utility nominal frequency that is added to the output of the regulator then outputted as the grid frequency. After the loop filter, whose output is the grid frequency, a voltage-controlled oscillator (VCO) is applied. This is usually an integrator, which gives the phase locked angle of the grid θ as output.

4. MODELICA IMPLEMENTATION

4.1 PHOTOVOLTAIC CELLS MODEL

The photovoltaic cell was simulated on three stages together to form the photovoltaic model simulation:

1) The first stage is expressing the relation of the input temperature and sun radiation and converting them to the current and voltage generated accordingly and getting finally to construct the generated IV curve in this stage taking into consideration the main effect of change in temperature and sun radiation on the output results.

2)The second stage is the cell 2 lines char, which is an intermediate stage connecting stage one temperature, solar radiation inputs and the main values calculated to represent the characteristics of the IV curve (open circuit voltage, short circuit current, alpha, and the corresponding voltage to alpha) with stage three and the main function of this stage is introducing the system power equilibrium of the solar radiation which is generating useful electrical power and also part of the solar radiation is not transformed to electricity resulting in thermal heat generation at the surface of the solar cell module and increase of the ambient temperature of the cell in general.

3) The third stage is the cell 2 lines and it uses the data from the previous two stages and connecting them together to give the final model that represents the PV cell through the third stage block only, which contains directly the input values of the solar radiation, the input temperature and the output positive and negative pins hiding all the details inside the previous 2 stages.

As shown in the above figure (13) the three stages together Modelica diagram and gives at the end only the needed points to connect the PV cell with the outer world like amount of solar radiation intensity, thermal heat exchange through the heat port and other electrical systems through the positive and negative pins.

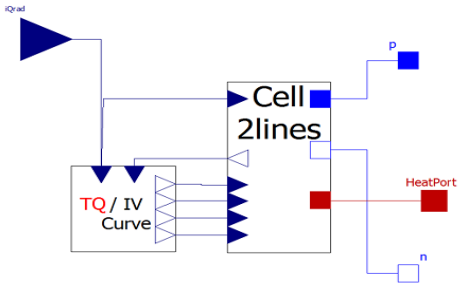

Fig.13: Cell 2 lines Modelica diagram

Now just few parameters need to be inserted before simulation of the model as shown in the following figure (14).

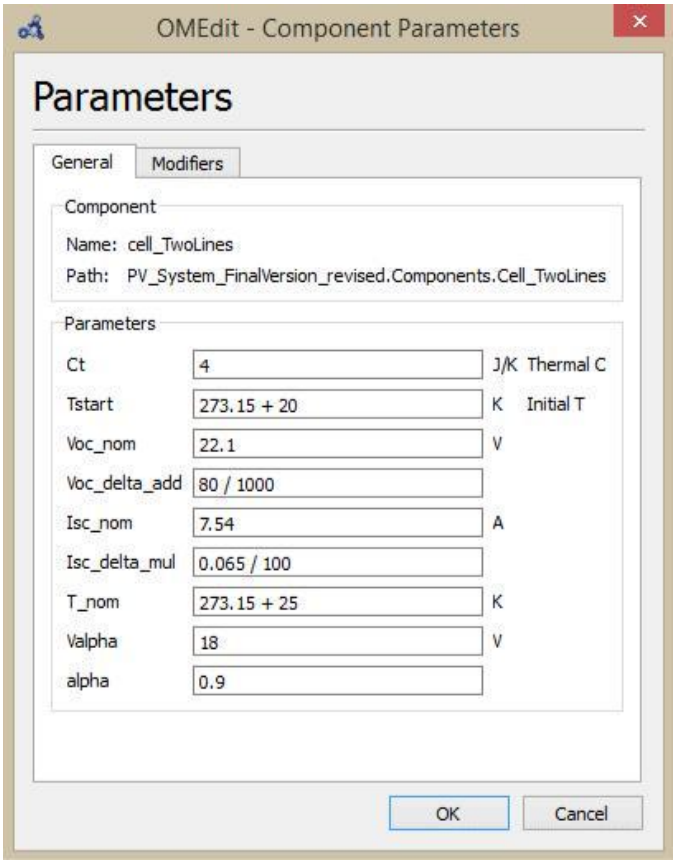

FIG. 14: Cell 2 lines parameters

Since no real experiment was executed in this thesis, the values of parameters were found in the suitable literature sources. Through reading the BP solar data sheet of BP 3125 the parameters values were found as shown in the figure (13) below.

Typical Electrical Characteristics	BP 3125
Maximum Power (P_{max})	125W
Warranted minimum power	119W
Voltage at P_{max} (V_{mp})	17.6V
Current at P_{max} (I_{mp})	7.1A
Short circuit current (I_{sc})	7.54A
Open circuit voltage (V_{oc})	22.1V
Temperature coefficient of I_{sc}	(0.065±0.015)%/K
Temperature coefficient of V_{oc}	-(80±10)mV/K
Temperature coefficient of P_{max}	-(0.5±0.05)%/K
NOCT (Air 20ºC; Sun 0.8kW/m²; wind speed 1m/s)	47±2ºC
Maximum series fuse rating	15A (BP 3125S) / 20A (BP 3125U)
Maximum system voltage	1000V (IEC 61215 rating)
	1000V (TÜV Rheinland rating)

Standard test conditions - irradiance of 1000W/m² at an AM1.5G solar spectrum and a temperature of 25°C.

FIG.13: BP 3125 datasheet

The configuration used for testing the Cell 2 lines module as shown in figure (14) below.

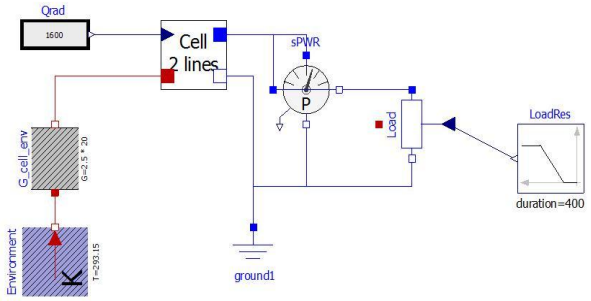

FIG. 14: cell 2 lines test configuration

4.2 BATTERY MODEL

The internal construction of the battery is divided into two main parts; the electrical and thermal parts.

First the electrical part consists of the positive and negative pins, simulated with a controlled voltage source in series with a small resistance, and is interfaced with a USB device, simulated with a resistive load.

While the thermal part is composed of the heat port this is also connected to the heat ports of both resistances of the model Rb and R_L to indicate the amount of heat generated inside the model due to chemical reactions and represent the battery temperature to be connected through a thermal conductor to the temperature of the environment at the end which is expressed be the Cplate to simulate the heat transfer exchange effect.

And more details about the battery model are shown in the figure (15) below.

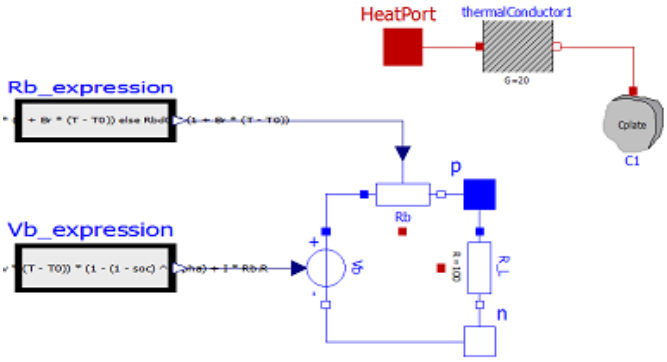

Fig .15: Battery Modelica diagram

And finally the parameters needed for the model simulation are in the figure (16).

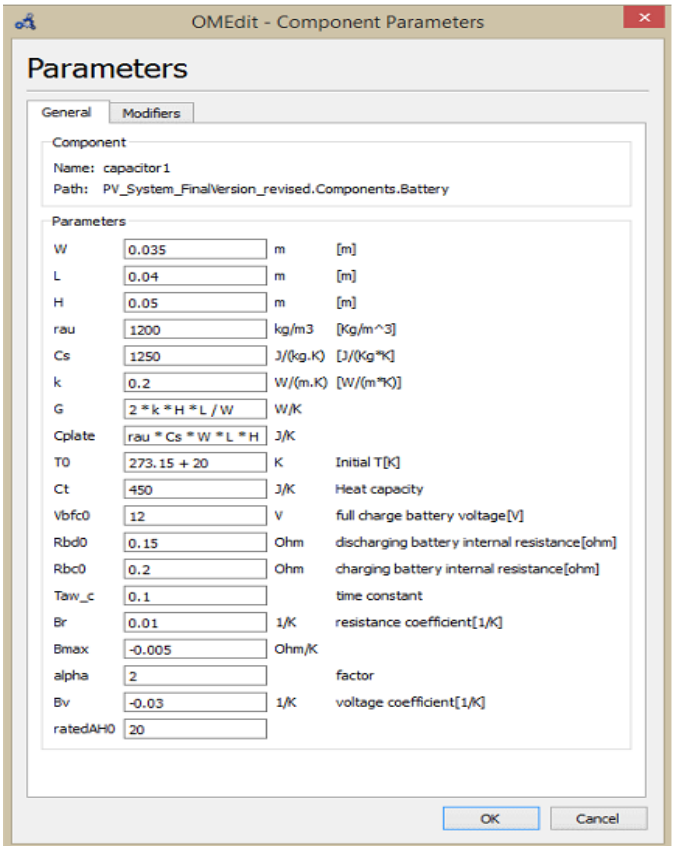

Fig.16: Battery Parameters

4.3 Inverter Model NVERTER MODEL

The model is done in a simple way to express the relation between input DC power and output AC power including the efficiency of the inverter.

$$Pac = Pdc \times \eta$$

Then the Power on each side was declared in details, in the DC side power is a relationship of the variable DC current and voltages.

$$Pdc = Vdc \times Idc$$

While at AC side the power is a function of imaginary and real voltages and currents defined in the phase's pins as described through the equations:

$$Pac = Vre \times Ire + Vim \times Iim$$

Where, Vre is the real voltage, Ire is the imaginary voltage, Vim is the imaginary voltage, Iim is the imaginary current. Then the relation between control inputs to form the AC output voltage is described

$$Vim = Vac \times sin\delta + (R + 2\pi fL) \times \sqrt{Ire^2 + Iim^2} \times \sin\left(arctan\left(\frac{X}{R}\right) + \frac{\pi}{2}\right)$$

through the equations:

For completing the model simulation more parameter values figure (17)are needed to be assigned for R and L that were chosen of small values (0.1) as the Inverter has very low impedance, while Frequency was fixed to 50 Hz and Efficiency as 0.95 %.

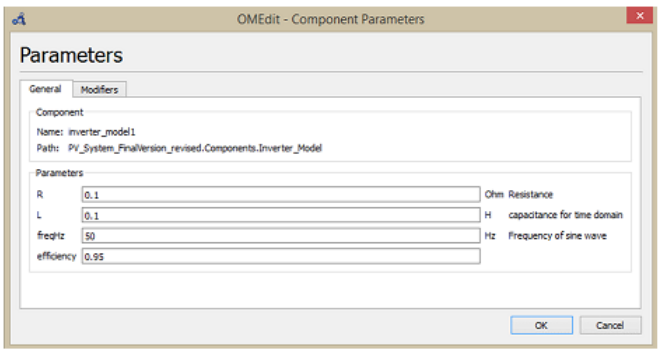

Fig.17: inverter parameters

4.4 Controller

All power systems must include a control strategy that describes the interactions between its components. The use of battery as a storage form implies thus the presence of a charge controller.

The charge controller is used to manage the energy flow to PV system, batteries and loads by collecting information on the battery voltage and knowing the maximum and minimum values acceptable for the battery voltage. There are two main operating modes for the controller:

1) Normal operating condition, when the battery voltage fluctuates between maximum and minimum voltages.

2) Overcharge or over-discharge condition, which occur when the battery voltage reaches some critical values.

To protect the battery against an excessive charge, the PV arrays are disconnected from the system, when the terminal voltage increases above a certain threshold V_{max_off} and when the current required by the load is less than the current delivered by the PV arrays. PV arrays are connected again when the terminal voltage decreases below a certain value V_{max_on}. This can be done by using a switch with a hysteresis cycle, as illustrated in figure (18).

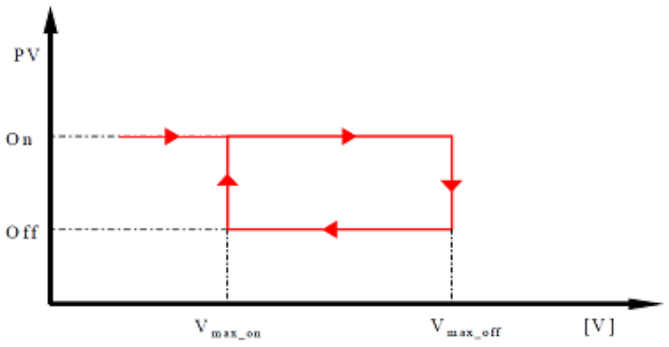

Fig. 18: operating principle of an overcharge protector

To protect the battery against excessive discharge, the load is disconnected when the terminal voltage falls below a certain threshold V_{min_off} and when the current required by the load is bigger than the current delivered by the PV arrays. The load is reconnected to the system when the terminal voltage is above a certain value V_{min_on}, using a switch with a hysteresis cycle, as shown in figure (19).

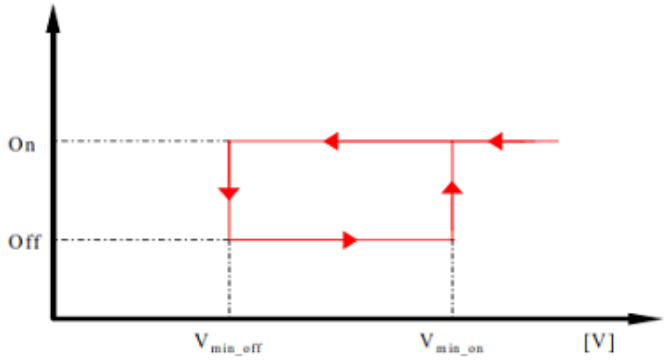

Fig .19: operating principle of an discharge protector

The steps in the modelling of the controller process are summarized in Table below:

	Constraint	Command
(1)	If $V>V_{max\_off}$ and $I_{load}<I_{pv}$	Disconnect PV arrays from the system
(2)	If command (1) is done and $V<V_{max\_on}$	Reconnect PV arrays to the system
(3)	If $V<V_{min\_off}$ and $I_{load}>I_{pv}$	Disconnect the load from the system
(4)	If command (3) is done and $V>V_{min\_on}$	Reconnect the load to the system

Summary of controller process – Table

Three controllers are available in the library. MPPT Controller provides a simple implementation of the Perturb and Observe (P&O) algorithm for MPP tracking. The power output from the PV array is measured and an increase or decrease of the DC bus voltage is effected. If the power decreases, the opposite action is effected in the next step.

If the power increases, the same action is repeated.

If the power doesn't change (i.e. it's below a certain threshold), voltage is not changed.

This algorithm is not the most efficient or effective, but it has reasonable performance and is easy to implement.

Iverter1ph Current Controller figure (20-a) provides current control in the synchronous reference frame for a 1-phase inverter. This is achieved by calculating the d_q coordinates of the output current, using a PI controller for each coordinate. With this setup, the d coordinate can be used to control the active power and the q coordinate to control the reactive power. The output of this block is the duty cycle, which can then drive an inverter.

%name PV control Inverter1phCompleteController figure (20-b) build upon the previ-ous by adding an outer voltage control loop to the active power control (id),using an MPPT Controller block. It also adds a PLL block for synchronization with the grid.

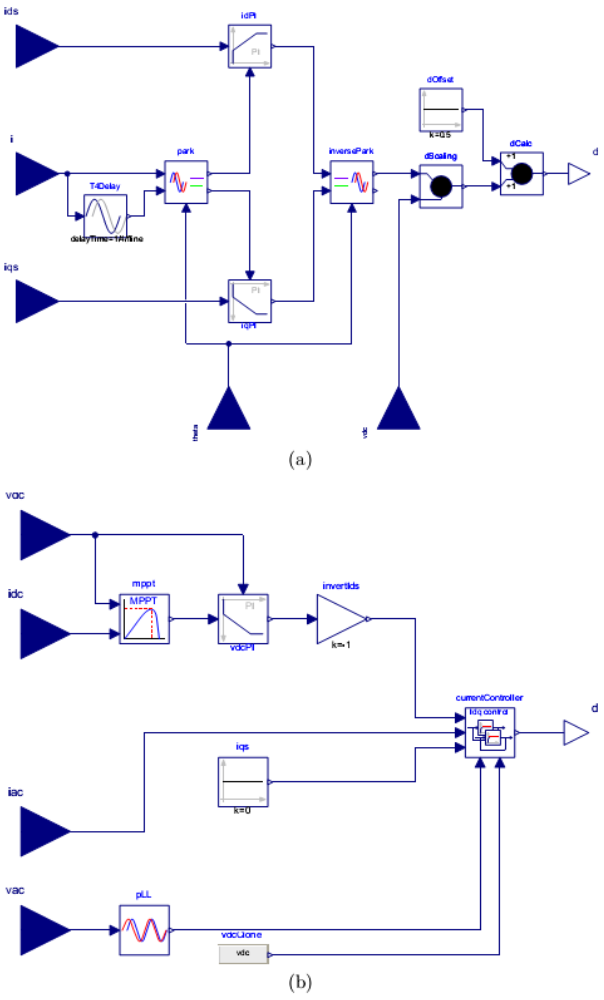

Fig .**20**: Inverter controllers in Control. Assemblies

5. Result

This example provides a model of a very simple single-phase grid-tied photovoltaic system figure (21). On the DC side, a single PV panel is modelled with PVArray placed in series with a small resistor. A capacitor is used to model the capacitance placed in the DC bus of the inverter. On the AC side, the output filter is modelled with an inductor in series with a small resistor. The grid is modelled with an ideal voltage source.

The control is implemented with an instance of the Inverter1phCompleteCon-troller, available as an assembly in the Control package. For more details on this block.

The simulation is configured to run for 28 s. The grid frequency is set at 50Hz, which makes this time quite long compared with the time-scale of the grid dynamics. On the other hand, the MPPT control and corresponding power changes are on the scale of seconds, which is why the stop time is set at that value, in order to observe some interesting dynamics at that level.

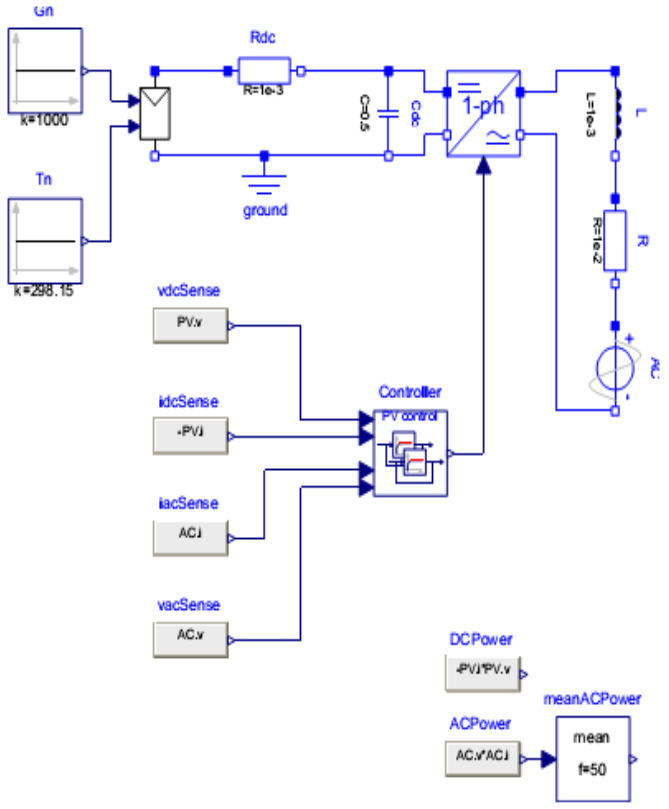

Fig .21: Model of a very simple single-phase grid-tied photovoltaic system

Figure (22-a) displays the variation of the DC voltage imposed by the inverter, controlled by the MPPT and current controller loop. The steps in voltage correspond to the adjustments that the MPPT controller is making (following the P&O algorithm). These steps are translated into the power steps shown in Figure (22-b). Eventually, since the irradiance and ambient temperature conditions are not changing, the controller finds the MPP. This is close to the 200W of the default PV Array parameter values. Finally, Figure (22-c) displays a close-up of the output voltage and current, to emphasize the fact that the output current is controlled to stay in phase with the grid voltage, providing only active power to the grid.

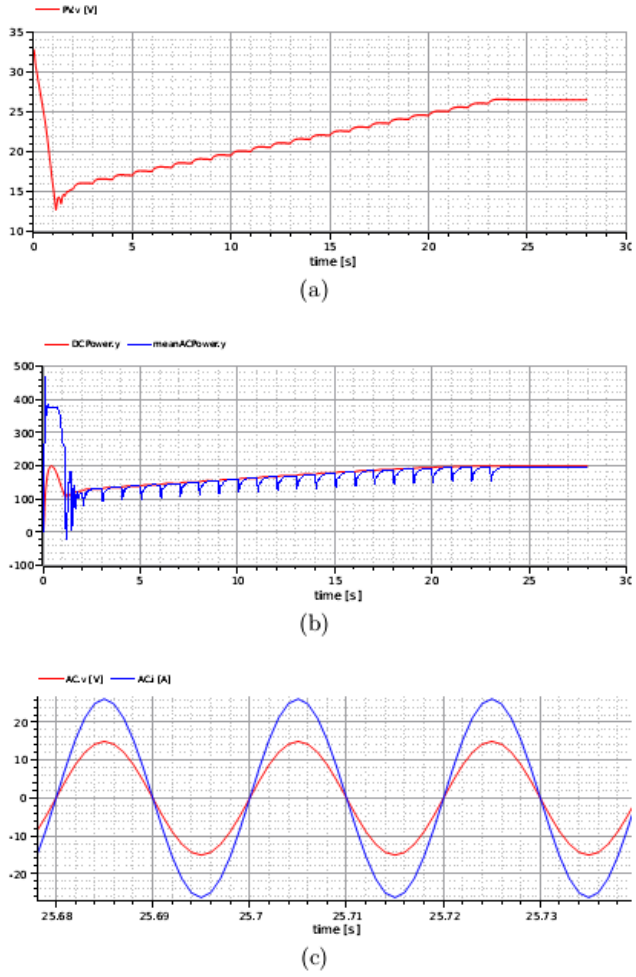

Fig.22: PVInverter1phSynch simulation results: (a) PV array voltage, (b) inputand output power, (c) grid voltage and output current.

6. Conclusions

The decision to create a Modelica library for photovoltaic systems with a focus on power electronics and with a model for battery energy storage was based on the belief that these technologies will be at the center of an energy abundant future.

Providing tools for scientists and engineers to develop these technologies is one strategy to accelerate the advent of this future.

Modelica supports this purpose perfectly. With it's open non-proprietary nature, it's readily available to users and tool developers without costly fees or complicated license agreements. This kind of openness can drive a thriving ecosystem that eventually creates solutions

that surpass the commercially available traditional ones.

Modelica is also developed with compensability and reusability in mind, with the inclusion of object orientation and causal equation based modelling and connection of components. This makes it easy to create models integrating several physical domains.

Following is conclusions that were drawn from the work performed in this paper:

• All of the relevant behaviors of the elements included in the original scope of the library (photovoltaic array, power electronics and battery energy storage) could be modelled with the use of equivalent circuits. Many physical processes where left out, but the goal of providing models for inverter control development is achieved with this level of modelling.

• The switch network concept becomes really valuable when modelling the power electronics components, since it provides a generalized and compostable structure for the modelling of power converters. Coupled with Modelica language features like *redeclare,* it also provides a way of creating very user-friendly models that can be instantiated as switched or averaged variants.

• Taking into account the implicit size and time scales that were assumed as a consequence of the goal of the library (supporting inverter control development),it seems that the modelling of battery energy storage might not even be required.

• Regression testing in Dymola can provide a very quick and convenient way to verify the correctness of models as changes are made. To be fair, this is true when considering changes that don't substantially change the functionality of a given model and assuming the reference data generated represents a run of a correct model. Regression tests will be most helpful in mature projects in which changes mainly correspond to optimizations of the code.

7. REFERENCES

[1] Huan-Liang Tsai, Ci-Siang Tu, and Yi-Jie Su, Development of Generalized Photovoltaic model using matlab-simulink.

[2] Jihad Bou Merhi, Jana Chalak, and Joya Zeitouny, Estimation of Battery Internal Parameters.

[3] Anca D. Hansen, Poul Sørensen, Lars H. Hansen and Henrik Bindner, Models for a stand-alone PV system.

[4] S. W. Angrist, Direct Energy Conversion, Allyn and Bacon, Inc., 4 th edition, 1982, pp. 177-227.

[5] J. C. H. Phang, D. S. H. Chan, and J. R. Philips, "Accurate analytical method for the extraction of solar cell model parameters," Electronics Letters, vol. 20, no. 10, 1984, pp.406-408.

[6] Massimo Ceraolo, Tarun Huria, Rechargeable lithium battery energy storage systems for vehicular applications, PHD thesis.

[7] R. A. Huggins, "Advanced batteries: materials science aspect", Springer, 2008. ISBN 0-3877-6423-2

[8]Abdelhalim Zekry, A. Alshazly, A. Abdelrahman, Simulation and implementation of grid-connected inverters, International Journal of Computer Applications (0975 – 8887), Volume 60– No.4, December 2012.

[9] Pallavee Bhatnagar, R.K. Nema, Maximum power point tracking control techniques; State-of-the-art in photovoltaic applications.

[10] Z.M. Salameh, M.A. Casacca, W.A. Lynch, "A Mathematical Model for Lead-Acid Batteries", IEEE Trans. Energy Conversion, vol. 7, issue 1, pp. 93-97, Mar. 1992, doi:10.1109/60.124547.

[11] M. Chen, G.A. Rincon-Mora, "Accurate electrical battery model capable of predicting Runtime and I_V Performance," IEEE Trans. Energy Conversion, vol. 21, no. 2, pp. 504-511, Jun. 2006, doi:10.1109/TEC.2006.874229.

[12] Ceraolo, M., "New Dynamical Models of Lead-Acid Batteries", IEEE Trans. Power Systems, vol. 15, no. 4, pp. 1184-1190, Nov. 2000, doi:10.1109/59.898088.

[13] Kobayashi K, Takano I, Sawada Y. A study on a two stage maximum power point tracking control of a photovoltaic system under partially shaded insolation conditions. In: IEEE Power Engineering Society General Meeting 2612–2617.2003.

[14] Al Nabulsi A, Dhaouadi R. Efficiency optimization of a DSP-based standalone PV system using fuzzy logic and dual-MPPT control. IEEE Transactions on Industrial Informatics 2012; 8(3):573–84.

[15] Kashif Ishaque, Zainal Salam, A review of maximum power point tracking techniques of PV system for uniform insolation and partial shading condition.

[16] Olaf Enge, Christoph Clauß, Peter Schneider, Peter Schwarz, Quasi-stationary AC Analysis using Phasor description With Modelica.